Journal of Medicinal Chemistry

Article

4-Aminoquinoline Antimalarials Containing a Benzylmethylpyridylmethylamine Group are Active against Drug Resistant *Plasmodium falciparum* and Exhibit Oral Activity in Mice

Mukesh C. Joshi, John Okombo, Samkele Nsumiwa, Jeffrey Ndove, Dale Taylor, Lubbe Wiesner, Roger Hunter, Kelly Chibale, and Timothy J Egan

J. Med. Chem., **Just Accepted Manuscript** • DOI: 10.1021/acs.jmedchem.7b01537 • Publication Date (Web): 29 Nov 2017

ACS Publications

Journal of Medicinal Chemistry is published by the American Chemical Society. 1155 Sixteenth Street N.W., Washington, DC 20036

4-Aminoquinoline Antimalarials Containing a Benzylmethylpyridylmethylamine Group are Active against Drug Resistant *Plasmodium falciparum* and Exhibit Oral Activity in Mice

Mukesh C. Joshi,[†‡||] John Okombo,[†‡] Samkele Nsumiwa,[†] Jeffrey Ndove,[§] Dale Taylor,[§] Lubbe Wiesner,[§] Roger Hunter,[†] Kelly Chibale[†⊥] and Timothy J. Egan[†]*

[†] Department of Chemistry, University of Cape Town, Rondebosch 7701, South Africa

[⊥] South African Medical Research Council Drug Discovery and Development Research Unit, Department of Chemistry and Institute of Infectious Disease and Molecular Medicine, University of Cape Town, Rondebosch 7701, South Africa

[§] Department of Medicine, Division of Clinical Pharmacology, University of Cape Town, Observatory, 7925, South Africa

[‡] these authors contributed equally to the work.

[||] current address: Motilal Nehru College, Benito Juarez Marg, South Campus, University of Delhi, New Delhi-110043, India

ABSTRACT: Emergence of drug resistant *Plasmodium falciparum* including artemisinin-tolerant parasites highlights the need for new antimalarials. We have previously shown that dibemequines, 4-amino-7-chloroquinolines with dibenzylmethylamine (dibemethin) side chains, are efficacious. In this study, analogues in which the terminal phenyl group of the dibemethin was replaced with a 2-pyridyl group and the 4-amino-7-chloroquinoline was either maintained or replaced with a 4-aminoquinoline-7-carbonitrile were synthesized in an effort to improve drug-likeness. These compounds exhibited significantly improved solubility and decreased lipophilicity and were potent against chloroquine-sensitive (NF54) and resistant (Dd2 and 7G8) *P. falciparum* strains with 5/6 having IC_{50}s <100 nM against the NF54 strain. All inhibited both β-hematin (synthetic hemozoin) formation and hemozoin formation in the parasite. Parasitemia was reduced by over 90% in *P. berghei*-infected mice in 4/7 derivatives following oral dosing at 4 × 30 mg/kg, with microsomal metabolic stability data suggesting that this could be attributed to highly active metabolites.

INTRODUCTION

Inhibition of the heme detoxification pathway in *Plasmodium falciparum* is an ideal target for antimalarial drugs owing to its critical role in parasite survival, absence of a human equivalent and non-genomic derivation (hence immutability). Chloroquine (CQ) and a number of related aminoquinolines are proposed to target this pathway, inhibiting the formation of inert crystalline hemozoin.[1-3] However, the efficacy of many of these quinolines has been compromised to a greater or lesser extent by the spread of CQ-resistant (CQR) parasites which harbor mutations in the chloroquine resistance transporter gene (*Pfcrt*) whose cognate protein (alongside other transporters) mediates drug extrusion from the parasite digestive vacuole (DV).[4, 5] At present, artemisinin combination therapy (ACT) constitutes the recommended treatment option against malaria and though still largely effective, there is a growing body of evidence that artemisinin-tolerant *P. falciparum* parasite strains are emerging, and consequently threatening the therapeutic utility of the ACT regimen.[6, 7] Therefore, novel strategies to address the challenge of antimalarial resistance and develop cheap new drugs with good safety profiles are urgently needed.

One approach to discovery of novel and potent antimalarial agents involves structural re-engineering of existing CQ-like drugs by, for instance, coupling them to resistance reversers. Seminal work on this strategy has been reported by Peyton and co-workers, in which they proposed preservation of the fundamental pharmacophore for heme-binding (4-aminoquinoline), inhibition of hemozoin formation (4-amino-7-chloroquinoline) and drug accumulation (a tertiary amino group in the side-chain) in covalent linkage with the pharmacophore for a chloroquine chemosensitizing or resistance reversal agent (RA), namely two suitably positioned aromatic groups with an amino group separated by a short chain.[8-10] The rationale behind the potency of these molecules is that the cellular transport machinery would fail to recognize the hybrid leading to vacuolar accumulation, or the molecule would

directly target the function of the efflux protein(s) thus blocking its extrusion. Indeed, the feasibility of this approach has since been interrogated by other groups who have generated various modifications of such compounds. For instance, conjugates based on pentacycloundecylamine, dihydropyrimidinone, astemizole and acridines with potent activity against CQR parasite strains have been reported.[11-14] Recently, our group also synthesized and evaluated dibemequine analogues containing a 4-amino-7-chloroquinoline nucleus with a dibenzylmethylamine side chain. These compounds exhibited strong in vitro antiplasmodial and in vivo antimalarial efficacy and notably, were further able to inhibit PfCRT-mediated drug extrusion from the parasite DV.[15]

In an attempt to further improve the drug-like properties of these compounds we have now made various structural alterations to the prototype molecule (Figure 1) to afford new analogues. First, the terminal phenyl ring in the dibenzylmethylamine side group was replaced with an *o*-pyridyl ring with the aim of improving aqueous solubility via introduction of an extra hydrogen bond acceptor. This was additionally expected to potentially improve vacuolar drug accumulation through pH trapping. Secondly, the chloro- substituent at carbon 7 (C7) on the 4-aminoquinoline core was replaced by a nitrile group to afford analogues with lower molecular weight (MW) and lipophilicity while still retaining β-hematin inhibition activity that critically depends on the substituent at this position.[16] This, we envisaged, would lower the potential for hERG channel inhibition (a frequent liability among aromatic weak bases such as these) and improve druggability by improving solubility.[17] Finally, one of the original parent series compounds, **1**, was prepared as a hydrochloride salt since its corresponding free base had previously been shown to possess low intrinsic solubility, which limited oral bioavailability. Here, we report potent in vitro activity, improved physicochemical properties and retention of antimalarial efficacy of these modified dibemequines in vivo as a further validation of the reversed-CQ strategy. In addition, we

present data on metabolite identification studies on of these compounds and a mechanistic investigation with respect to targeting the hemoglobin degradation pathway.

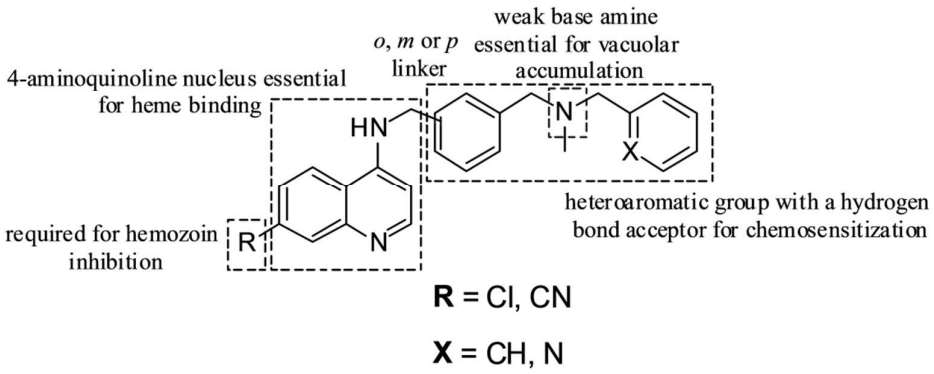

Figure 1: Prototype compound showing the structure activity relationship (SAR) that was explored to afford various analogues evaluated in this study. **1**: R = Cl, X = CH, linker *m*; **2**: R = Cl, X = N, linker *o*; **3**: R = Cl, X = N, linker *m*; **4**: R = Cl, X = N, linker *p*; **5**: R = CN, X = N, linker *o*; **6**: R = CN, X = N, linker *m*; **7**: R = CN, X = N, linker *p*.

CHEMISTRY

The target molecules (**2** – **7**) were synthesized by reaction of the appropriate *N*-(n-(aminomethyl)benzyl)-*N*-methyl-1-(pyridine-2-yl)methanamine where n = 2 – 4 containing an *o*, *m* or *p* linker group (**8**, **9** and **10** respectively) with an excess of commercially available 4,7-dichloroquinoline or 4-chloro-7-cyanoquinoline in anhydrous *N*-methyl-2-pyrrolidone in the presence of anhydrous K_2CO_3 with triethylamine as a base (Scheme 1).[15] Each reaction was carried out in sealed cycloaddition tubes under a N_2 atmosphere with a gradual increase of temperature to 90 °C. Once this temperature was reached, the reaction was allowed to stir for an additional 48 h. The products were then extracted from an alkaline aqueous solution into ethyl acetate and purified by column chromatography to afford modest yields (23 to 46%). All products were characterized by infrared, ^{1}H and ^{13}C NMR, and mass spectrometry.

Solid intermediates were further characterized by elemental combustion analysis. All final products were subjected to high-resolution mass spectrometry to confirm identity, and HPLC to confirm purity (see Supporting Information for further details).

8, **9** and **10** were prepared in three steps (Scheme 1). First, 1-(azidomethyl)-2, 3 and 4-(bromomethyl)benzenes (**11**, **12** and **13**) were prepared from the appropriate dibromoxylene (**14**, **15** and **16**) via a substitution reaction with sodium azide as previously described.[18] The appropriate azido intermediate was then reacted with *N*-methyl-1-(pyridin-2-yl)methanamine (**17**) to afford a series of *N*-(n-(azidomethyl)benzyl)-N-methyl-1-(pyridin-2-yl)methanamines (n = 2 – 4) (**18, 19, 20**) using anhydrous K_2CO_3 as base in anhydrous acetonitrile at 0 °C, followed by overnight reflux. These were then converted to the corresponding *N*-(n-(aminomethyl)benzyl)-*N*-methyl-1-(pyridine-2-yl)methanamine (n = 2 – 4) via a Staudinger reduction involving reaction with PPh_3 in THF for 30 min at room temperature, followed by the addition of water and reflux for an additional 6-10 h. All the intermediates were purified by SiO_2 gel column chromatography in a good to moderate yield.

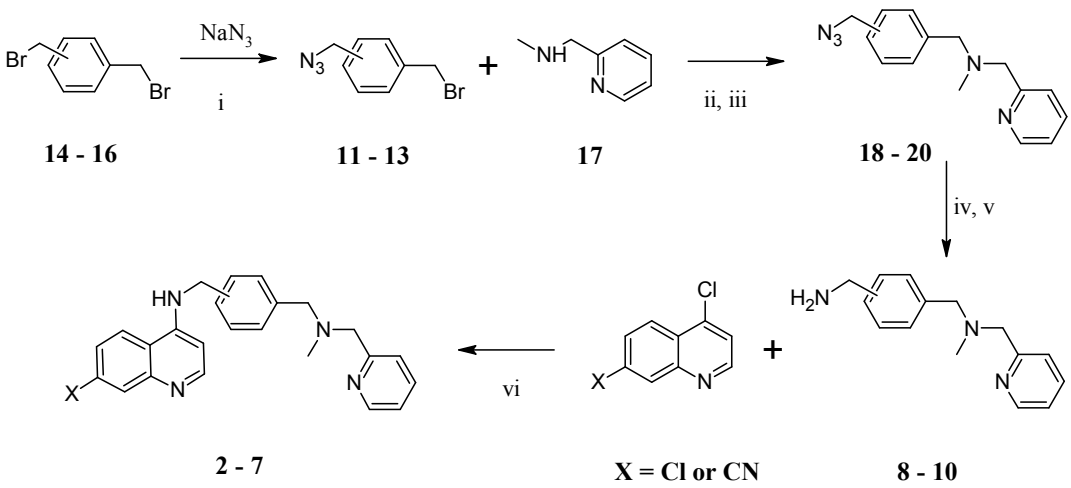

Scheme 1: Reagents and conditions: (i) DMF, RT, 16 h; (ii) CH_3CN, K_2CO_3 (1.5 equiv.), 0 °C; (iii) Δ, 16 h; (iv) PPh_3 (1.2 equiv.), THF, RT, 0.5 h; (v) H_2O, Δ, 6 h; (vi) K_2CO_3, TEA, N_2, 90 °C, 48 h (X = Cl, CN).

PHYSICOCHEMICAL AND BIOLOGICAL PROFILING

Solubility, Membrane Permeability and Lipophilicity. As an initial measure of the effectiveness of the structural modifications in improving the drug-like characteristics of this series, solubility, permeability and partitioning properties of the new derivatives were measured. The compounds generally exhibited moderate to high solubility in aqueous medium at pH 6.5 (Table 1) ranging from 52 to 197 μM. With the exception of **3** and **6**, replacement of the terminal phenyl ring with a pyridyl ring substantially increases solubility of the free base relative to the parent hydrochloride compound **1·HCl**. In view of their weak base properties, they exist predominantly in their ionized protonated state at lower pH, with the consequence that they are likely to stay in solution under assay conditions. Replacement of the chloro with a cyano group at C7 on the quinoline ring did not seem to further influence solubility.

Replacement of the terminal phenyl ring with a pyridyl group caused a small, but significant decrease in permeability relative to the parent compound **1**, consistent with the decreased lipophilicity of the ring. Nonetheless, the derivatives all still showed high membrane permeability at pH 6.5 in the PAMPA assay ($\log P_{app} > -5$) and are predicted to permeate the gastrointestinal wall via passive diffusion efficiently (Table 1). Replacement of the 7-Cl group with a CN group had little effect on permeability.

The series exhibited moderately lipophilic experimental partition coefficients, with $\log D_{7.4}$ values ranging between 2.47 and 3.80. Under acidic conditions (pH 5.0), all compounds had a substantially reduced log*D*, consistent with ionization of the weakly basic groups. The pyridodibemequines had somewhat lower $\log D_{5.0}$ than the parent compound **1**, with the 7-cyano derivatives showing no substantial difference from the 7-Cl derivatives.

Table1: Physicochemical profile of the seven test compounds and standards.

Compound	Kinetic Solubility pH 6.5 (μM)	Permeability Average Log P_{app} (SD)		Partition Coefficient	
		pH4.0	pH6.5	Log$D_{7.4}$	Log$D_{5.0}$
1.HCl	51.8	ND	-3.60 (0.16)	3.56	1.33
2	164.7	-6.14 (0.34)	-4.56 (0.03)	3.79	0.90
3	59.8	-3.81 (0.03)	-4.10 (0.26)	2.47	0.82
4	196.6	-3.85 (0.32)	-4.56 (0.10)	2.85	0.84
5	172.4	-6.03 (0.12)	-4.01 (0.06)	3.80	0.81
6	72.4	ND	-3.60 (0.16)	2.75	0.85
7	143.5	-4.51 (0.40)	-4.60 (0.04)	2.84	1.00
Reserpine	<5				
Hydrocortisone	>150			1.50	
Verapamil				2.50	
Warfarin		-3.70 (0.35)	-3.80 (0.35)		
Propranolol		-5.90 (0.28)	-4.40 (0.28)		

ND: not determined

hERG Channel Inhibition. A concern with lipophilic weak base compounds is their potential cardiotoxicity, with QT prolongation caused by inhibition of hERG channels. Gleeson has shown that compounds with MW below 400 and cLogP below 4 are statistically less likely to exhibit hERG toxicity.[17] In accordance with this, predicted hERG IC_{50} values (Table 2) obtained using StarDrop™ software showed an improvement in predicted pIC_{50} (6.22 – 6.43) compared to the parent compound **1** (6.55). The predicted pIC_{50} values compare favorably with the clinical antimalarials CQ (6.00) and lumefantrine (6.64) and are substantially lower than that of halofantrine (7.37), an antimalarial with known cardiotoxicity. One of the compounds, **2**, was selected for experimental measurement of

hERG inhibition in CHO cells with stable hERG expression. This compound exhibited an experimental hERG IC_{50} of 0.87 ± 0.08 μM (pIC_{50} = 6.06), comparable to verapamil used as a control (IC_{50} = 0.56 ± 0.08 μM). The observed value was in good agreement with the predicted pIC_{50} of 6.28, supporting the prediction that these compounds have lower hERG liability than halofantrine, but that it would nonetheless remain a concern for this series.

Potential Vacuolar Accumulation. The vacuolar accumulation ratio (VAR) and lipid accumulation ratio (LAR) have been implicated in predicting the activity of hemozoin inhibiting antimalarials and in determining cross-resistance with CQ. For this reason, experimental Log*D* values were used to calculate the VAR and LAR as described previously by Warhurst and co-workers.[19] These values are presented in Table 2, together with MW and cLog*P* data. A notable feature is that the VAR values are more than two orders of magnitude lower than that reported by Warhurst for CQ (143,482), while the LAR values are more than an order of magnitude larger than CQ.[19, 20] The three compounds with the largest VAR values (**1**, **2** and **5**) also have the highest LAR values. This does not correspond to a high cLog*P* in the case of **2** or **5** as these values are comparable to the other compounds in the respective series (**3** and **4**; **6** and **7** respectively). The increased LAR must therefore arise from a lower pK_a in these compounds. Notably, both have an *ortho* substituent arrangement in the side chain allowing for intramolecular hydrogen bonding between the 4-amino group on the quinoline and the deprotonated tertiary amino group in the side chain.

Table 2: Predicted VAR, LAR, MW, cLog*P* and predicted hERG inhibition *p*IC50 (–logIC_{50}) of test compounds and five reference antimalarial compounds

Compound	VAR	LAR	Molecular Weight	cLogP	hERG pIC_{50}
1.HCl	170	3630	439.4	6.36	6.55
2	776	6165	402.9	4.81	6.28
3	45	295	402.9	4.86	6.23
4	102	708	402.9	4.86	6.43
5	977	6309	395.5	3.66	6.23
6	79	562	395.5	3.82	6.22
7	69	692	395.5	3.71	6.39
CQ	ND	ND	319.8	3.81	6.00
Lumefantrine	ND	ND	528.9	9.12	6.64
Mefloquine	ND	ND	378.3	3.95	5.72
Halofantrine	ND	ND	500.4	7.65	7.37
***N*-desbutylhalofantrine**	ND	ND	444.3	6.08	6.52

VAR = vacuolar accumulation ratio = antilog(log$D_{7.4}$ – log$D_{5.0}$). LAR = lipid accumulation ratio = antilog(log$D_{7.4}$); hERG *p*IC_{50}s were obtained from StarDrop™ while cLog*P* values were computed with ChemDraw™ Ultra 14.0; ND = Not determined

Activity Against *P. falciparum* in Vitro. All compounds showed potent antiplasmodial activity in the nanomolar range against CQS and CQR parasite strains (Table 3). Chloro-substituted analogues had higher potency across all strains than cyano, an unsurprising observation as it has been previously shown that halogens exert optimum influence at 7-

position on the quinoline ring due to their strong lipophilicity and a moderately strong electron-withdrawing capacity.[16] Against Dd2, all compounds were more active than CQ while only **1**, **3**, **4** and **7** were more potent against the 7G8 strain. The slightly weaker activity seen with 7G8 could possibly be attributed to differences in PfCRT arising from one or more of the seven amino acids that differ between the Dd2 and 7G8 forms of PfCRT expressed in the two strains or differential regulation in the pathways that compensate for these mutations in these strains.[21]

There was no indication of cross-resistance between the test compounds and CQ in the two strains of CQR parasites as indicated by their resistance indices which were all below 5 in the test compounds, but above 20 for CQ. This low cross-resistance with CQ could be a result of the incorporation of the pyridodibemequine moiety as a side chain. This side chain could bind to and subsequently inhibit transport of the molecule by $PfCRT^{CQR}$ or bind to $PfCRT^{CQR}$ but simply fail to be translocated because of the altered side chain, or the altered side chain may result in the molecule not being recognized at all.

These compounds also showed low cytotoxicity in a mammalian cell line (CHO cells) with a selectivity index range between 146 and 740 (Table 3), highlighting the specificity of their activity. By contrast, emetine, a potent inhibitor of protein synthesis in eukaryotic cells, exhibited cellular toxicity at extremely low concentrations. There was no discernible trend in cytotoxicity attributable to any structural features of the molecules, perhaps due to the limited number of derivatives investigated.

Table 3: Antiplasmodial activity, cytotoxicity profiles and β-hematin inhibition activity of the series

Compound	In Vitro $_{IC50}$ (nM)					Cytotoxicity		βHIA_{IC50} (SD)
	NF54	Dd2	7G8	$R.I_{Dd2}$ [a]	$R.I_{7G8}$	CHO_{IC50} (µM)	S.I[b]	(µM)
1.HCl	14.4	44.5	69.6	3.1	4.8	9.5	660	13.4 (1.8)
2	54.4	136.6	184.3	2.5	3.4	40.2	740	17.9 (3.2)
3	30.1	124.0	83.8	4.1	2.8	8.3	275	20.8 (0.6)
4	38.5	150.7	114.2	3.9	3.0	15.7	408	17.2 (0.3)
5	126.6	162.0	307.1	1.3	2.4	27.6	218	16.6 (0.4)
6	79.1	89.4	151.0	1.1	1.9	50.6	639	16.7 (0.1)
7	76.4	145.5	134.0	1.9	1.8	11.2	146	24.8 (2.1)
CQ [c]	8.3	226.4	150.3	27.3	21.9	ND	ND	26.1 (3.4)
Artesunate	5.6	14.3	7.7	2.6	1.4	ND	ND	ND
Emetine	ND	ND	ND	ND	ND	0.095	ND	ND

[a] R.I = Resistance index = [IC_{50} CQR strain] / [IC_{50} CQS strain]; [b] SI= Selectivity index = [IC_{50} CHO] / [IC_{50} PfNF54]; ND = Not Determined. βHIA = β-hematin inhibition activity; [c] Chloroquine diphosphate salt.

In view of the fact that they encompass the CQ pharmacophore, these compounds were evaluated for their ability to inhibit formation of β-hematin using a detergent-based assay that mimics the conditions of the parasite acidic DV. All compounds were found to be more potent inhibitors of β-hematin formation than CQ (Table 3). Analysis of the relationship between antiplasmodial activity and inhibition of β-hematin formation reveals no correlation

between parasite IC_{50} and β-hematin inhibition IC_{50}. On the other hand, we observed a significant increase in in vitro activity (pIC_{50}) with increasing cLog*P* in the CQS strain (R^2 = 0.91, P = 0.008, see Figure 2a). A similar correlation was also observed in both CQR strains, but neither reached significance at the 95% confidence level (Dd2: R^2 = 0.51, P = 0.071; 7G8: R^2 = 0.55, P = 0.057). These findings suggest that the potency of these quinolines likely hinges more on access to the vacuolar compartment than on strength of inhibition of hemozoin. This may reflect the larger variations in cLog*P* values than in βHIA IC_{50}s in this series.

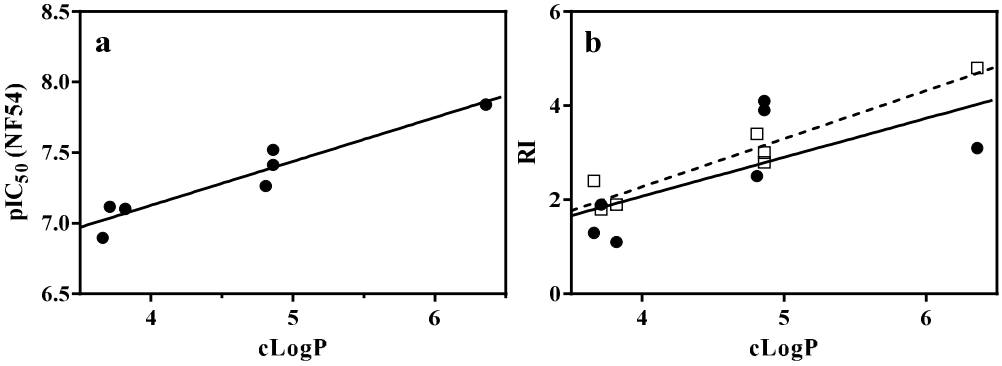

Figure 2: Plot showing correlation between: **(a)** biological activity (pIC_{50}) and lipophilicity (cLog*P*) in the CQS NF54 strain and (b) RI and cLogP in the two CQR strains, Dd2 (solid circles and line) and 7G8 (open squares and dashed line).

While no correlations were seen between parasite growth IC_{50} or RI and either the VAR or LAR, a trend of increasing RI with cLog*P* was seen in both the Dd2 and 7G8 strains relative to NF54, albeit only significant in the case of the 7G8 strain (R^2 = 0.91, P = 0.0007) and not the Dd2 strain (R^2 = 0.44, P = 0.10). Interestingly, in this series the effect of high lipophilicity seems to be to reduce activity in the CQR strains, the opposite of what has been reported for other quinolines.[19]

Intracellular Hemozoin Inhibition. To establish whether this series of compounds actually inhibits intracellular hemozoin formation in *P. falciparum*, we used a cellular heme fractionation assay to determine whether or not there was a dose-dependent effect of the compounds on the various heme components (hemoglobin, free heme and hemozoin) in the parasite.[22] Exposure of synchronized ring stage parasites to the test compounds for 32 h caused statistically significant dose-dependent decreases in the fraction of total heme present as hemozoin and a corresponding increase in the fractions of "free" or exchangeable heme for all the compounds in a manner similar to CQ (Figure 3). This dose-dependent profile persisted for all compounds when the amount of heme per cell, rather than proportion, was determined by dividing the heme measurement (expressed as mass of heme Fe) by cell count obtained through flow cytometry (Supplementary Figure 2). Parasite survival curves overlaid on the free heme Fe per cell showed that an increase in free heme corresponded to a decrease in parasite survival (Supplementary Figure 2). There was no significant perturbation in the quantities free heme or hemozoin in parasites exposed to pyrimethamine, which is a non-hemozoin inhibiting control.

In Vivo Antimalarial Efficacy. In view of the favorable in vitro activity and safety profiles, we went on to screen a selection of compounds for in vivo oral activity against *Plasmodium berghei* using the Peters 4 day suppressive test performed at 30 mg/kg doses over 1-4 days post-infection.[23] All the compounds tested, except for **2**, **5** and **6** achieved >90% suppression of parasitemia according to this protocol, which is comparable with CQ (Table 4). For comparison, the activity of the free base of **1** reported in our previous study is also shown.[15] The new series appears to exhibit similar efficacy.

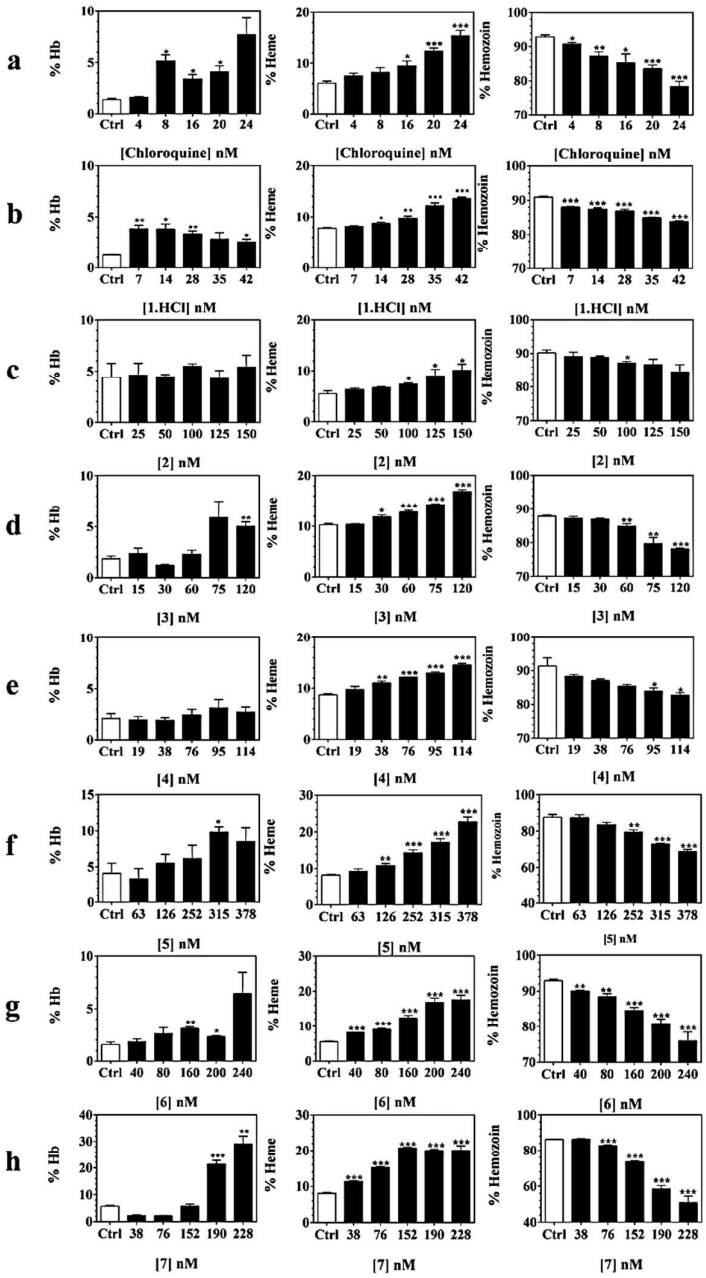

Figure 3: Effects of dose of CQ (a), the parent dibemequine **1.HCl** (b) and modified dibemequines **2** (c), **3** (d), **4** (e), **5** (f), **6** (g) and **7** (h) on hemoglobin (left panels), free heme (middle panels) and hemozoin (right) panels in the CQS NF54 strain of *P. falciparum*. Increase relative to control in Hb and heme and decrease in hemozoin: * $P < 0.05$; ** $P < 0.01$; *** $P < 0.001$.

Table 4: In vivo antimalarial activity of test compounds in *P. berghei*-infected mice.

Compound	Dose (mg/kg)	% Parasitized RBCs	% of Control
1.HCl	4 × 30	0.26 ± 0.05	97.5
2	4 × 30	1.8 ± 0.3	82.4
3	4 × 30	0.22 ± 0.11	97.8
4	4 × 30	0.88 ± 0.28	91.4
5	4 × 30	5.4 ± 1.5	47.1
6	4 × 30	1.3 ± 1.2	87.3
7	4 × 30	0.20 ± 0.18	98.0
CQ	4 × 30	0.9 ± 0.1	91.2
1[a]	3 × 30	0.10 ± 0.02	99.9
Untreated		10.2 ± 1.1	

[a] Reference 15.

Metabolic Stability and Putative Metabolite Identification. Finally, the metabolic stability of the entire series was tested. All the compounds exhibited very short degradation half-lives after single point incubation with mouse liver microsomes and high hepatic clearance ratios (>0.90) suggesting notable susceptibility to hepatic metabolism (Table 5).

These compounds were thus all metabolically unstable with fractions metabolized comparable to the metabolically labile standard midazolam. Varying the arrangement of the side chain linker from the *ortho*- to the *meta*- or *para*- position had no significant effect on compound stability as is sometimes expected for such changes arising from steric effects on enzyme access to metabolically labile sites on the molecule. This high metabolic susceptibility has implications on in vivo activity as plasma exposure is likely to be poor and

bioavailability low following dosing. To further understand this rapid compound clearance, mass spectrometry scan data from the metabolic stability assay for each compound was screened for the presence of fragments corresponding to putative metabolites and routes/sites of metabolism. The metabolite profiles of all compounds appeared to be similar, with *N*-dealkylation on the tertiary amine seemingly the predominant pathway (metabolites 1 and 2). Other metabolites detected included products arising from oxidation of the quinoline core or pyridyl ring (metabolite 5), *N*-dealkylation together with oxidative deamination (metabolite 6) as well as aldehyde reduction (metabolite 3) and oxidation of the aldehyde to carboxylic acid (metabolite 4) as depicted in Figure 4.

Table 5: In vitro metabolism in mouse liver microsomes

Compound	**% remaining (after 30 min)**	**Projected $t_{1/2}$ (min)**	**Intrinsic Clearance CL (mL/min/kg)**	**Predicted E_H[a]**
1.HCl	3.57	6.15	1106.62	0.92
2	2.32	5.49	1223.91	0.93
3	2.96	5.89	1138.53	0.93
4	2.08	5.35	1250.06	0.93
5	2.08	5.35	1249.33	0.93
6	1.91	5.10	1348.68	0.94
7	3.63	6.22	1101.28	0.90
Midazolam[b]	1.33	4.74	1424.93	0.94
MMV390048[b]	93.55	172.25	42.03	0.32

[a] Fraction metabolized; [b] metabolically labile and inert standards respectively.

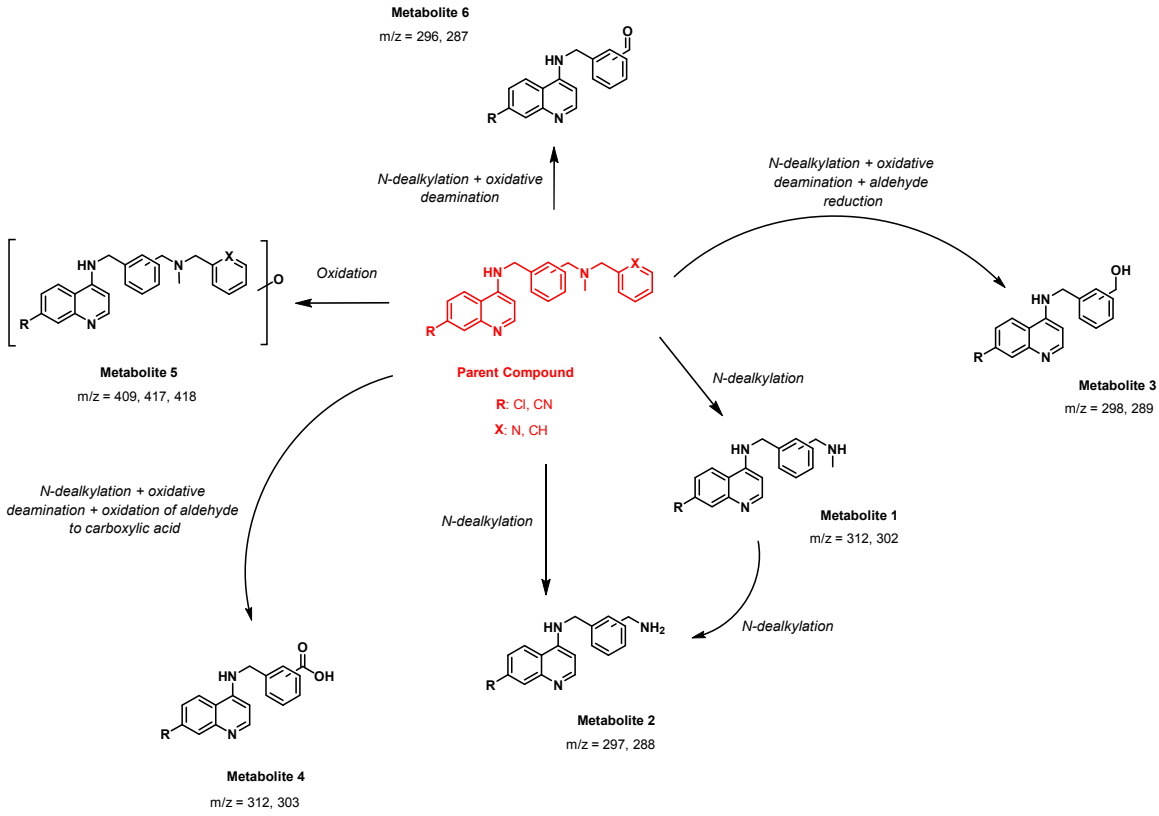

Figure 4: Proposed metabolic fragmentation pattern of the representative compounds with putative metabolite structures and masses based on mass spectrometric measurements.

DISCUSSION

The hypothesis that replacement of the terminal phenyl ring in the dibemequine series with an *o*-pyridyl ring and of the 7-Cl group on the quinoline with a 7-CN group would not substantially reduce activity against *Plasmodium* either in vitro or in vivo was borne out in this study. Compounds bearing a 7-Cl group had IC_{50} values against the CQS NF54 strain of *P. falciparum* about twice that of the parent dibemequines, while the 7-CN bearing derivatives exhibited IC_{50}s about four times higher than the parent compounds. In a four day Peters test at 30 mg/kg, all the compounds measured were indistinguishable from each other, from the parent dibemequine **1** and from **CQ**. Resistance indices (RIs) for the CQR Dd2 and

7G8 strains were comparable to, or better than the parent compound **1.HCl**. All were below 5, suggesting no significant cross-resistance with CQ which had RIs above 20. All of the compounds exhibited relatively low cytotoxicity against mammalian (CHO) cells, with IC_{50}s close to, or above 10 μM. Selectivity indices for *P. falciparum* were all above 100 for the NF54 strain. Thus, these derivatives retained their excellent activity and selectivity against malaria parasites.

The prediction that these compounds would exhibit improved drug-like properties over the parent compounds was to some extent supported. All showed an improvement in kinetic solubility relative to **1**.HCl, albeit a small improvement. Similarly, small improvements in predicted hERG liability were also seen. It should be noted that none of these improvements were significant and the predicted hERG pIC_{50} of the parent compound **1** was itself not that much different from CQ and was considerably lower than halofantrine. Overall, the success of this strategy with regard to solubility and hERG liability was marginal and came at the cost of somewhat reduced permeability.

All of the compounds were found to inhibit β-hematin formation in the NP-40 detergent-based assay. The range of IC_{50} values was, however, very narrow (16.6 – 24.8 μM) and comparable to both the parent compound **1**.HCl and CQ (13.4 and 26.1 μM). No correlation was found between IC_{50}s for β-hematin and parasite growth inhibition. Rather, activity against the parasite is strongly correlated with cLog*P*. This indicates that the activity of compounds is predominantly determined by access to the interior of the cell as has been observed before. Nonetheless, measurement of "free" heme and hemozoin levels in treated parasites showed that "free" heme levels clearly rise and hemozoin levels drop with increasing dose and that parasite survival is correlated with the increase in "free" heme, strongly suggesting that hemozoin inhibition is the basis of activity of these compounds. The

effects of the very small differences in β-hematin inhibition activity in these compounds may in fact be masked by the much larger influence of lipophilicity on access to the target.

In view of the good in vivo activity of these compounds, their high level of metabolic instability in liver microsomes was noteworthy and suggested the activity was due to the metabolites rather than the parent. The principal metabolites (1 and 2) retain the key pharmacophore of the 4-aminoquinoline antimalarials, namely a 4-amino-7-chloroquinoline core with side chain bearing a basic amino group. We predicted that they are still likely to be β-hematin inhibitors and will inhibit hemozoin in the parasite. Interestingly, their lower MW and cLog*P* may in fact be beneficial for improved solubility. In view of this, we have gone on to synthesize a series of the predicted metabolites 1 and 2 from compounds **1** – **4**. These predicted metabolites retain the β-hematin inhibitory properties of the parent compounds with IC_{50} values <24 μM and are active against *P. falciparum* in culture, with IC_{50} values ranging between 9.2 and 25 nM in the metabolite 1 series and 9.8 – 231 nM in the metabolite 2 series in the NF54 strain. Cytotoxicity in CHO cells covers a range of IC_{50} values from 5.0 – 7.4 μM in metabolite series 1 and 10.7 – 168 μM in metabolite series 2. These data confirm that the metabolites are selectively strongly active against the parasite. Detailed studies are underway and will be reported in a further publication.

CONCLUSIONS

Replacement of the terminal phenyl ring in the dibemequines with a 2-pyridyl ring and replacement of the 7-Cl group with a 7-CN group resulted in a series of compounds that retained both in vitro and in vivo antimalarial activity, had acceptable parasite selectivity and minimal cross-resistance in CQR parasite strains. The resulting decrease in lipophilicity was associated with only a slight decrease in predicted and experimental hERG liability, but the

compounds were all highly metabolically labile. Indeed, the observed activity of these compounds in mice suggests that the metabolites are responsible for this in vivo activity.

EXPERIMENTAL SECTION

General Methods. Solvents, acids, and other commercially obtained chemicals were purchased from Kimix Chemicals or Sigma-Aldrich. Thin layer chromatography was used to monitor reactions using pre-coated silica gel plates (Merck F_{54} aluminum backed). Silica for column chromatography was obtained from Merck, South Africa. Melting points were determined using a Reichert-Jung Thermovar hot stage microscope and are uncorrected. ^{1}H and ^{13}C NMR spectra were recorded on a Varian Mercury spectrometer at 300 MHz or a Varian Unity spectrometer at 400 MHz in d^3-chloroform with references 7.26 ppm for ^{1}H and 77.00 ppm for ^{13}C. Infrared spectra were recorded on a Perkin-Elmer Paragon 1000 FT-IR spectrophotometer in the range 3600-800 cm^{-1}. Mass spectra were recorded on a VG Micromass 16F spectrometer operating at 70 eV with an accelerating voltage of 4 kV and a variable temperature source. Accurate mass determinations were performed on a Kratos Limited MS9/50 spectrometer. All mass spectra were obtained using electron-impact techniques. All final products were subjected to high resolution mass spectrometry to confirm identity and analytical HPLC to confirm purity using a Spectra Series HPLC with Phenomenex-Luna, 3 μm C18 column, with a run time of 13 min (see Supporting Information). Purity exceeded 95% in all cases. Synthesis of **1** was described in a previous publication.

Procedure for the Syntheses of the Pyridodibemequine Analogues 2 - 7. To a solution of the appropriate *N*-(n-(aminomethyl)benzyl)-*N*-methyl-1-(pyridin-2-yl)methanamine **8**, **9** or **10** (2.63 g, 13.28 mmol) in NMP (8 ml), was added dry K_2CO_3 (1.37 g, 9.96 mmol) and triethylamine (2.31 ml, 16.70 mmol) in a sealed tube at room temperature and stirred for 5-10

min under N_2 atmosphere. Then, 4,7-dichloroquinoline or 4-chloro-7-cyanoquinoline (0.8 g, 3.3 mmol) was added to the reaction mixture under N_2 atmosphere. After addition of the quinoline, the sealed tube was capped and put into an oil bath with gradually heating to 90 °C. Once the temperature reached 90 °C, the reaction was allowed to stir for 48 h. Progress was monitored by TLC using EtOAc: hexane (8: 2) as a mobile phase while UV, iodine and ninhydrin were used to monitor the spots. After completion of reaction, the mixture was allowed to cool to room temperature and then poured into saturated brine solution (60 ml) and extracted with EtOAc (5-6 times with 50 ml each). The organic layer was collected and dried over anhydrous $MgSO_4$ and excess organic solvent was removed under vacuum. The crude product was then purified by using SiO_2 gel column chromatography. EtOAc: petroleum ether (25 : 75 to 35 : 65) were used to remove unreacted 4,7-dichloroquinoline or 4-chloro-7-cyanoquinoline. Then using 40-70 % EtOAc in petroleum ether other unwanted impurities were separated. Finally pure EtOAc or EtOAc: trimethylamine (95: 5) were used to elute the product. Preparative TLC was used to further purify the products using EtOAc: MeOH: EtOH (90: 6: 4) as mobile phase as required. Finally purity was confirmed by HPLC.

7-Chloro-N-(2-((methyl(pyridin-2-ylmethyl)amino)methyl)benzyl)quinolin-4-amine (2). White solid powder (33%); m.p.: 125-127 °C; IR: 3241 (NH), 2922 (CH), 1578 (C=C), 1611 (C=N), 753 (C−N); ^{1}H NMR ($CDCl_3$, 300 MHz) δ 8.52 (1H, ddd, J = 6.0, 3.0 1.8 Hz), 8.46 (1H, d, J = 5.7 Hz), 8.02 (1H, d, J = 1.8 Hz), 7.76 (1H, d, J = 9.0 Hz), 7.57 (1H, td, J = 7.5, 1.8 Hz), 7.43-7.40 (1H, m), 7.34-7.26 (3H, m), 7.20-7.15 (2H, m), 7.06 (1H, dd, J = 9.0, 2.1 Hz), 6.56 (1H, d, J = 5.7 Hz), 4.49 (2H, d, J = 5.4 Hz), 3.77 (2H, s), 3.70 (2H, s), 2.19 (3H, s); ^{13}C NMR ($CDCl_3$/CD_3OD (4 drops), 101 MHz) δ 158.0, 151.1, 150.8, 149.4, 148.5, 137.1, 137.0, 136.4, 135.0, 132.0, 130.5, 128.3, 127.9, 127.8, 124.9, 123.8, 122.6, 122.4, 117.9, 99.0, 63.9, 61.3, 46.5, 42.3; HRMS *m/z* $[M + H]^+$ calcd for $C_{24}H_{24}ClN_4$ 403.1684, found 403.1682; HPLC purity: 97.7%.

7-Chloro-N-(3-((methyl(pyridin-2-ylmethyl)amino)methyl)benzyl)quinolin-4-amine (3). Light yellow solid (23%); m.p.: 50-52 °C; IR: 3272 (NH), 2924 (CH), 1611 (C=C), 1579 (C=N), 758 (C−N); ^{1}H NMR ($CDCl_3$, 300 MHz) δ 8.51 (1H, dd, *J* = 3.9, 0.6 Hz), 8.32 (1H, d, *J* = 6.0 Hz), 8.14 (1H, d, *J* = 9.0 Hz), 8.03 (1H, d, *J* = 2.1 Hz), 7.62 (1H, td, *J* = 7.5, 1.8 Hz), 7.44-7.15 (7H, m), 6.43 (1H, d, *J* = 6.0 Hz), 4.61 (2H, d, *J* = 4.5 Hz), 3.67 (2H, s), 3.60 (2H, s), 2.24 (3H, s); ^{13}C NMR ($CDCl_3$, 101 MHz) δ 159.5, 150.6, 150.5, 149.1, 147.9, 140.0, 137.1, 136.3, 135.6, 128.9, 128.6, 128.0, 127.8, 126.2, 125.7, 122.9, 121.9, 121.7, 117.1, 99.6, 63.3, 61.9, 47.6, 42.5; HRMS *m/z* $[M + H]^+$ calcd for $C_{24}H_{24}ClN_4$ 403.1684, found 403.1688; HPLC purity: 98.29%.

7-Chloro-N-(4-((methyl(pyridin-2-ylmethyl)amino)methyl)benzyl)quinolin-4-amine (4). Light yellow powder (36%); m.p.: 115-118 °C; IR: 3272 (NH), 2923 (CH), 1609 (C=C), 1578 (C=N), 758 (C−N); ^{1}H NMR ($CDCl_3$, 300 MHz) δ 8.54 (1H, ddd, *J* = 5.1, 1.8, 0.9 Hz), 8.37 (1H, d, *J* = 6.0 Hz), 8.07 (1H, d, *J* = 9.0 Hz), 8.01 (1H, d, *J* = 2.1 Hz), 7.69 (1H, td, *J* = 9.0, 1.8 Hz), 7.50 (1H, d, *J* = 7.8 Hz), 7.37-7.31 (5H, m), 7.18 (1H, ddd, *J* = 7.2, 4.8, 0.9 Hz), 6.44 (1H, d, *J* = 6.0 Hz), 4.58 (2H, d, *J* = 4.8 Hz), 3.69 (2H, s), 3.59 (2H, s), 2.24 (3H, s); ^{13}C NMR ($CDCl_3$, 101 MHz) δ 159.7, 150.7, 150.3, 149.1, 147.6, 139.0, 136.3, 135.8, 135.8, 129.6, 127.5, 127.5, 125.8, 123.0, 121.9, 121.8, 117.1, 99.5, 63.4, 61.7, 47.4, 42.5; HRMS *m/z* $[M + H]^+$ calcd for $C_{24}H_{24}ClN_4$ 403.1684, found 403.1682; HPLC purity: 98.6%.

4-((2-((Methyl(pyridin-2-ylmethyl)amino)methyl)benzyl)amino)quinoline-7-carbonitrile (5). Off white solid powder (46%); m.p.: 145-148 °C; IR: 3259 (NH), 2962 (CH), 2230 (C≡N), 1588 (C=N), 1572 (C=C), 754 (C−N); ^{1}H NMR ($CDCl_3$, 300 MHz) δ 8.55 (1H, d, *J* = 5.7 Hz), 8.51 (1H, dd, *J* = 5.7, 1.5 Hz), 8.36 (1H, d, *J* = 1.2 Hz), 7.99 (1H, d, *J* = 8.7 Hz), 7.61 (1H, td, *J* = 7.5, 1.8 Hz), 7.43-7.41 (1H, m), 7.31-7.18 (6H, m), 6.65 (1H, d, *J* = 5.7 Hz), 4.50 (2H, d, *J* = 5.4 Hz), 3.78 (2H, s), 3.71 (2H, s), 2.17 (3H, s); ^{13}C NMR ($CDCl_3$, 101 MHz) δ 158.1, 153.2, 151.2, 149.0, 146.2, 137.0, 136.7, 136.5, 133.2, 131.8,

129.5, 128.3, 127.9, 125.2, 124.2, 123.2, 122.7, 121.7, 118.2, 112.9, 100.5, 63.5, 61.1, 45.8, 42.1; HRMS *m/z* $[M + H]^+$ calcd for $C_{25}H_{24}N_5$ 394.2026, found 394.2032; HPLC purity: 96.0%.

4-((3-((Methyl(pyridin-2-ylmethyl)amino)methyl)benzyl)amino)quinoline-7-carbonitrile (6). Off white solid powder (34%); m.p.: 153-158 °C; IR: 3271 (NH), 2927 (CH), 2228 (C≡N), 1587 (C=N), 1570 (C=C), 756 (C−N); ^{1}H NMR ($CDCl_3$, 300 MHz) δ 8.58 (1H, d, *J* = 5.4 Hz), 8.53 (1H, d, *J* = 4.8 Hz), 8.34 (1H, s), 8.03 (1H, d, *J* = 8.4 Hz), 7.64 -7.18 (8H, m), 6.55 (1H, d, *J* = 5.4 Hz), 5.88 (1H, bs, NH), 4.56 (2H, d, *J* = 4.8 Hz), 3.74 (2H, s), 3.69 (2H, s), 2.31 (3H, s); ^{13}C NMR ($CDCl_3$/CD_3OD (3 drops) 101 MHz) δ 158.7, 151.9, 150.8, 148.7, 146.9, 139.1, 137.4, 137.1, 134.2, 128.9, 128.7, 128.0, 126.4, 125.5, 123.6, 122.7, 122.5, 121.6, 118.5, 113.0, 101.1, 62.7, 61.9, 47.2, 42.3; HRMS *m/z* $[M + H]^+$ calcd for $C_{25}H_{24}N_5$ 394.2026, found 394.2034; HPLC purity: 99.4%.

4-((4-((Methyl(pyridin-2-ylmethyl)amino)methyl)benzyl)amino)quinoline-7-carbonitrile (7). Off white solid powder (29%); m.p.: 152-155 °C; IR: 3289 (NH), 2661 (CH), 2228 (C≡N), 1588 (C=N), 1570 (C=C), 758 (C−N); ^{1}H NMR ($CDCl_3$, 300 MHz) δ 8.57 (2H, m), 8.35 (1H, s), 8.05 (1H, d, *J* = 8.7 Hz), 7.70 (1H, td, *J* = 7.8, 1.5 Hz), 7.57 – 7.50 (2H, m), 7.43 – 7.33 (4H, m), 7.20 (1H, dd, *J* = 6.7, 5.6 Hz), 6.55 (1H, d, *J* = 5.4 Hz), 6.08 (1H, br, s, N*H*), 4.56 (2H, d, *J* = 5.1 Hz), 3.75 (2H, s), 3.67 (2H, s), 2.30 (3H, s); ^{13}C NMR ($CDCl_3$/CD_3OD (3 drops) 101 MHz) δ 158.9, 151.6, 150.9, 148.6, 146.6, 138.1, 137.1, 136.2, 134.0, 129.7, 127.3, 125.5, 123.6, 122.7, 122.5, 121.5, 118.4, 113.0, 101.1, 62.9, 61.6, 47.0, 42.2, ; HRMS *m/z* $[M + H]^+$ calcd for $C_{25}H_{24}N_5$ 394.2026, found 394.2029;HPLC purity: 99.0%.

Procedure for the Syntheses of Amine Intermediates 8 - 10. To a stirred solution of the appropriate *N*-(n-(azidomethyl)benzyl)-*N*-methyl-1-(pyridin-2-yl)methanamine **18**, **19** or **20** (2.0 g, 7.49 mmol) in THF (30 ml) was added PPh_3 (1.57 g, 5.99 mmol) at room

temperature under nitrogen atmosphere and the reaction mixture was allowed to stir for additional 30 min. Water was added (6.79 ml, 376 mmol) and the reaction mixture was refluxed for 6-10 h. Reaction progress was monitored by TLC using EtOAc: MeOH : Et_3N (5 : 4 : 1) as a mobile phase and ninhydrin and iodine as stain. Excess THF was removed under high vacuum while the remaining water was removed as an azeotrope with toluene. The crude product was purified by SiO_2 gel column chromatography using EtOAc and petroleum ether as an eluent to remove impurities and finally the desired product was obtained using EtOAc : MeOH : Et_3N (85 : 10 : 5) as eluent.

***N*-(2-(Aminomethyl)benzyl)-*N*-methyl-1-(pyridin-2-yl)methanamine (8).** Dark brown liquid (1.40 g, 70%), ^{1}H NMR ($CDCl_3$, 300 MHz) δ 8.77 (1H, ddd, *J* = 4.8, 1.8, 0.9 Hz), 7.74 (1H, dd, *J* = 7.2, 1.5 Hz), 7.64 (1H, td, *J* = 7.8, 1.8 Hz), 7.38 – 7.16 (5H, m), 4.21 (2H, s), 3.68 (2H, s), 3.62 (2H, s), 2.25 (3H, s); ^{13}C NMR ($CDCl_3$, 101 MHz) δ 156.9, 150.2, 137.7, 136.7, 133.5, 133.1, 131.1, 129.0, 129.0, 123.4, 122.5, 62.0, 61.4, 42.2, 42.2; EI-MS *m/z* M^+ calcd for $C_{15}H_{19}N_3$ 241.16, found 241.05 (83).

***N*-(3-(Aminomethyl)benzyl)-*N*-methyl-1-(pyridin-2-yl)methanamine (9).** Light brown solid (1.63 g, 76%); ^{1}H NMR ($CDCl_3$, 300 MHz) δ 8.53 (1H, dd, *J* = 4.8, 0.9 Hz), 7.66 (1H, td, *J* = 7.8, 1.8 Hz), 7.47-7.23 (5H, m), 7.16 (1H, ddd, *J* = 7.5, 4.8, 0.9 Hz), 4.07 (2H, s), 3.60 (2H, s), 3.50 (2H, s), 2.13 (3H, s); ^{13}C NMR ($CDCl_3$, 101 MHz) δ 159.0, 149.0, 139.1, 136.6, 131.4, 129.1, 128.9, 128.7, 127.4, 123.1, 122.1, 63.3, 61.7, 44.3, 42.4; EI-MS *m/z* M^+ calcd for $C_{15}H_{19}N_3$ 241.16, found 241.06 (73); Anal. calc. for $C_{15}H_{19}N_3$: C, 74.65%; H, 7.94%; N, 17.41%. Found: C, 74.41%; H, 7.41%; N, 17.64%.

***N*-(4-(Aminomethyl)benzyl)-*N*-methyl-1-(pyridin-2-yl)methanamine (10).** Dark brown solid (1.85 g, 92%); ^{1}H NMR ($CDCl_3$, 300 MHz) δ 8.54 (1H, m), 7.68 (1H, td, *J* = 7.8, 2.1 Hz), 7.52-7.27 (5H, m), 7.16 (1H, m), 3.89 (2H, s), 3.69 (2H, s), 3.59 (2H, s), 2.25 (3H, s); ^{13}C NMR ($CDCl_3$, 101 MHz) δ 161.6, 149.0, 137.5, 136.4, 135.1, 129.1, 128.2, 123.0,

122.0, 63.3, 61.8, 42.5, 42.4; EI-MS *m/z* M^+ calcd for $C_{15}H_{19}N_3$ 241.16, found 241.05 (65); Anal. calc. for $C_{15}H_{19}N_3$: C, 74.65%; H, 7.94%; N, 17.41%. Found: C, 74.57%; H, 6.98%; N, 16.91%.

Procedure for the Synthesis of *N*-methyl-1-(pyridin-2-yl)methanamine (17). To a stirred solution of pyridine-2-caboxaldehyde (8.89 mL, 93.4 mmol) in MeOH (100 ml) at room temperature, 40% aq. methylamine (12.03 mL, 140 mmol) was added slowly and the reaction allowed to progress at 65 °C for 2 h. The reaction mixture was allowed to cool to 0 °C, then $NaBH_4$ (2.48 g, 65.4 mmol) was added slowly and reaction continued for 6 h at room temperature. Reaction progress was monitored by TLC. After completion of the reaction, the remaining solvent was removed under high vacuum. The crude reaction mixture was worked up by the addition of a saturated solution of aq. Na_2CO_3 and the product extracted into $CHCl_3$ (3 × 100 ml) and the organic extracts dried over anhydrous $MgSO_4$. The solvent was then removed under reduced pressure to give a crude product (11.8 g), which was chromatographed on silica-gel using 5% MeOH + 5% TEA + DCM as eluent. The product was dried under *vacuum* to give *N*-methyl-1-(pyridin-2-yl)methanamine as a yellow oil (9.2 g, 74%):[24] ^{1}H NMR (300 MHz, $CDCl_3$) δ 8.49 (dd, 1H, J = 4.8, 0.9 Hz), 7.55 (td, 1H, J = 7.5, 1.5 Hz), 7.25 (m, 1H), 7.10 (m, 1H), 3.70 (s, 2H), 2.35 (s, 3H); ^{13}C NMR ($CDCl_3$,75 MHz) δ 159.5, 149.2, 136.4, 122.3, 121.2, 60.00, 35.9. EI-MS *m/z* M^+ calcd for $C_7H_{10}N_2$ 122.08, found 122.08.

Procedure for the Syntheses of Azido Intermediates 18 – 20. The synthesis of 1-(azidomethyl)-2, 3 or 4-(bromomethyl)benzene intermediates (**11**, **12** and **13)** from commercially available dibromoxylenes **14**, **15** and **16** has been previously described.[18] To a stirred solution of crude **11**, **12** or **13** (2.5 g, 11.01 mmol) and K_2CO_3 (3.78 g, 27.53 mmol) in anhydrous acetonitrile (50 ml) at 0 °C, was added *N*-methyl-1-(pyridin-2-yl)methanamine (**17**, 1.07 g, 8.81 mmol) and the reaction heated and allowed to progress under reflux

overnight. Acetonitrile was then removed under reduced pressure and the reaction mixture worked up with ethyl acetate (100 ml) and saturated aqueous Na_2CO_3 (3 × 50 ml), dried ($MgSO_4$) and concentrated under vacuum. The crude product was purified by SiO_2 gel column chromatography using mixtures of ethyl acetate: hexane (50: 50) to (80: 20) as eluent to give the *N*-(n-(azidomethyl)benzyl)-*N*-methyl-1-(pyridin-2-yl)methanamines (n = 2 – 4).

***N*-(2-(Azidomethyl)benzyl)-*N*-methyl-1-(pyridin-2-yl)methanamine (18).** Dark yellow oil (1.45 g, 73%); ^{1}H NMR ($CDCl_3$, 300 MHz) δ 8.58 (dd, 1H, *J* = 4.8, 0.9 Hz), 7.70 (td, 1H, *J* = 7.5, 1.5 Hz), 7.51 – 7.48 (m, 2H), 7.33 - 7.20 (m, 2H), 4.51 (s, 2H), 3.75 (s, 2H), 3.65 (s, 2H), 2.22 (s, 3H); ^{13}C NMR ($CDCl_3$, 101 MHz) δ 158.5, 149.0, 136.9, 136.5, 135.0 130.9, 129.5, 128.2, 127.8, 123.1, 122.1, 63.7. 59.9, 52.1, 42.4; EI-MS *m/z* M^+ calcd for $C_{15}H_{17}N_5$ 267.15, found 267.23 (75).

***N*-(3-(Azidomethyl)benzyl)-*N*-methyl-1-(pyridin-2-yl)methanamine (19).** Light yellow liquid (1.90 g, 96%); ^{1}H NMR ($CDCl_3$, 300 MHz) δ 8.58 (dd, 1H, *J* = 4.8, 0.9 Hz), 7.70 (td, 1H, *J* = 7.5, 1.5 Hz), 7.56 (d, 1H, *J* = 7.8 Hz), 7.40 – 7.18 (m, 5H), 4.35 (s, 2H), 3.81 (s, 2H), 3.73 (s, 2H), 2.33 (s, 3H); ^{13}C NMR ($CDCl_3$, 101 MHz) δ 158.8, 149.0, 139.0, 136.4, 135.5, 128.9, 128.7, 128.7, 126.9, 123.0, 122.0, 63.3, 61.7, 54.7, 42.4; EI-MS *m/z* M^+ calcd for $C_{15}H_{17}N_5$ 267.15, found 267.08 (66).

***N*-(4-(Azidomethyl)benzyl)-*N*-methyl-1-(pyridin-2-yl)methanamine (20).** Light yellow liquid (1.62 g, 60%); ^{1}H NMR ($CDCl_3$, 300 MHz) δ 8.58 (1H, dt, *J* = 4.8 0.9 Hz), 7.70 (1H, td, *J* = 7.8, 1.8 Hz), 7.58 (1H, d, *J* = 7.8 Hz), 7.47 (2H, d, *J* = 8.1 Hz), 7.31-7.26 (2H, m), 7.21 (1H, m), 4.29 (2H, s), 3.84 (2H, s), 3.78 (2H, s), 2.35 (3H, s); ^{13}C NMR ($CDCl_3$, 101 MHz) δ 158.3, 149.0, 138.0, 136.4, 134.5, 129.4, 128.2, 123.0, 122.0, 63.3, 61.6, 54.6, 42.4; EI-MS *m/z* M^+ calcd for $C_{15}H_{17}N_5$ 267.15, found 267.05 (72).

In Vitro Antiplasmodial Activity Tests using pLDH. The pLDH method for measuring parasite survival was based on that of Makler et al.[25] All parasite strains were acquired from

MR4 (Malaria Research and Reference reagent Resource Centre, Manassas, VA). Briefly, the assay procedure involved preparation of respective stock solutions of CQ diphosphate and test compounds to 2 mg/mL in distilled water (for CQ) and 100% DMSO (for test compounds) then stored at -20 °C and further dilutions prepared on the day of the experiment. Synchronized trophozoite-stage cultures of NF54 (CQS), Dd2 (CQR) and 7G8 (CQR) were prepared to 2% parasitemia and 2% hematocrit. Compounds were tested at starting concentrations of 10,000 ng/mL (1,000 ng/mL for CQ), which were then serially diluted 2-fold in complete medium to give 10 concentrations with final volumes of 200 µL in each well. Plates were covered with a sterile lid, placed in a gas chamber and incubated at 37 °C for 48 hours after which 100 µL of MalStat reagent was added to a new plate and 15 µL of re-suspended culture added to each well of this plate followed by addition of 25 µL of NBT (nitro blue tetrazolium chloride). The plates were kept in the dark for about 10 min to fully develop and absorbance measured at 620 nm on a microplate reader. Raw data were exported to Microsoft Excel and dose-response analysis performed in GraphPad Prism v.6 (GraphPad Software Inc., La Jolla, USA).

In vitro Cytotoxicity Assay. The 3-(4,5-dimethylthiazol-2-yl)-2,5-diphenyltetrazoliumbromide (MTT)-assay was used to screen compounds for *in vitro* cytotoxicity against Chinese Hamster Ovarian (CHO) mammalian cell-lines as previously described.[26] Briefly, test compounds were first prepared to a 20 mg/mL stock solution in 100% DMSO followed by further dilutions in complete medium. The initial concentration of the compounds was 100 µg/mL, which was serially diluted in complete medium with 10-fold dilutions to give 6 concentrations, the lowest being 0.001 µg/mL. Emetine was used as the reference drug in this experiment and the same dilution technique was applied to the control, and testing was performed in triplicate on each occasion. The 50% inhibitory concentration

(IC_{50}) values were obtained from full dose-response curves, using non-linear dose-response curve fitting analysis via GraphPad Prism v.6 (GraphPad Software Inc., La Jolla, USA).

In vivo Peters' Suppressive 4 Day Test. The CQS *P. berghei* (ANKA strain) was used to assess in vivo anti-malarial efficacy of the test compounds. The parasites were maintained in a C57BL/6 mouse by inoculation with 250 µl of a 1:1 (v/v) suspension of erythrocytes infected with *P. berghei* in phosphate buffered saline (PBS). On the day of the experiment the host mouse was anaesthetized intraperitoneally with a mixture of ketamine (120 mg/kg) and xylazine (16 mg/kg). Whole blood from the host mouse was drawn by cardiac puncture into a Vacuette® heparin tube and a suspension of *P. berghei* parasitized erythrocytes (1×10^7) in PBS was prepared and the test mice were infected with 200 µL of this suspension intraperitoneally.

The curative potential of the test compounds was evaluated using Peters' 4-day test as described elsewhere.[23] Briefly, the mice were dosed orally at 30 mg/kg 2 h post-infection and for three consecutive days (D_0 to D_3). CQ was used as a reference drug and was also dosed orally at 30 mg/kg. The control group of mice was also dosed orally with PBS. Parasitemia was determined from the third day (D_4) by preparing thin blood films from the tail of each mouse and the smears were fixed with methanol and stained with Giemsa. Equations 1 and 2 were used to calculate % parasitemia and reduction.

$$\%\, parasitemia = \frac{no.of\ parasitized\ RBCs}{Total\ no.of\ RBCs} \times 100 \qquad 1$$

$$\%\, reduction\ = \frac{parasitemia\ of\ placebo - parasitemia\ of\ test\ compound}{parasitemia\ of\ placebo} \times 100 \qquad 2$$

Parasite heme fractionation assay. The parasite heme fractionation assay examines the dose-dependent effect (if any) of an inhibitor on the fate of total heme in the parasite as previously described.[3, 22] Briefly, cultures were synchronized at 48-h intervals with 5%

(wt/vol) sorbitol, and ring-stage parasites incubated with the test drugs at various multiples of their IC_{50}s. RBCs were then harvested after 32 h, and the trophozoites were isolated with 0.05% (wt/vol) saponin and washed with 1× PBS (pH 7.5) to remove traces of the RBC hemoglobin. RBCs and trophozoites were quantified in these samples using a hemocytometer and flow cytometry. The contents of the trophozoite pellet were then released by hypotonic lysis and sonication. Following centrifugation, the supernatants corresponding to membrane-soluble hemoglobin fraction were treated with 4% (wt/vol) SDS and 2.5% (vol/vol) pyridine. The pellets were again treated with 4% SDS, 25% pyridine, sonicated, and centrifuged. Supernatants corresponding to the 'free' heme fraction were then carefully recovered. The remaining pellets (hemozoin fraction) were then solubilized in 4% SDS, 0.3 M NaOH and then neutralized with 0.3 M HCl, sonicated, and treated with 25% pyridine. The UV-visible spectrum of each heme fraction as an Fe(III) heme-pyridine complex was measured using a multiwell plate reader (Spectramax 340PC; Molecular Devices). The total amount of each heme species was quantified using a heme standard curve whereby the mass of each heme Fe species per trophozoite was calculated by dividing the total amount of each heme species by the corresponding number of parasites in that fraction as determined by flow cytometry (Combrinck et al, 2015).[22] Statistical comparisons were made using Students' t-test on GraphPad Prism v.6 (GraphPad Software Inc., La Jolla, USA).

hERG Toxicity Computational Prediction. StarDrop™ was used to predict hERG pIC_{50}s of the compounds whereby molecules were imported into the analysis software in spatial data file (sdf) format and the hERG pIC_{50} directly predicted. CQ, dihydroartemisinin, halofantrine and *N*-desbutylhalofantrine, all of whose predicted ranges of pIC_{50}s are known, were used as control.

hERG Toxicity Experimental Determination. Experimental analysis was performed on the QPatch gigaseal automated patch clamp platform whereby CHO cells stably expressing hERG protein were prepared for assays using proprietary dissociation protocols designed to optimise cell health, yield and assay quality. Test compound (**2**) and verapamil hydrochloride (positive control) were screened at four concentrations (0.3, 1, 3 and 10 μM) against a minimum of three separate CHO cells. The percent inhibition values from each cell were used to construct concentration-response curves employing a four parameter logistic fit with 0 and 100% inhibition levels fixed at very low and very high concentrations, respectively, and a free Hill slope factor. The IC_{50} and Hill coefficient were then determined, with only data with Hill slopes within $0.5 < nH < 2.0$ included. The IC_{50} data was then reported as the mean ± standard deviation (S.D.) of at least 3 separate cells ($n \geq 3$).

Kinetic Solubility. The kinetic solubility assay was performed using a miniaturized shake flask method as previously described.[27] Briefly, 10 mM stock solutions of each of the test compounds were used to prepare calibration standards (10 - 220 μM) in DMSO, and to spike (1:50) duplicate aqueous samples of FaSSIF (simulating fasting state bio-relevant media, pH 6.5), with a final DMSO concentration of 2%. After shaking for 2 h at 25 °C, the solutions were filtered and analyzed by means of HPLC-DAD (Agilent 1200 Rapid Resolution HPLC with a diode array detector). Best fit calibration curves were constructed using the calibration standards, which were used to determine the aqueous solubility of the samples.

Parallel Artificial Membrane Permeability Assay (PAMPA). The PAMPA assay was performed in triplicate in 96-well MultiScreen filter plates (Millipore, 0.4 μM PCTE membrane). Membrane filters were pre-coated with 5% hexadecane in hexane and allowed to dry prior to the assay. Membrane integrity marker, Lucifer yellow was added to the apical wells of the pre-coated MultiScreen plate donor/drug solutions containing test compound.

Phosphate buffer (pH 7.4) was added to the 96-well acceptor plate. 10 mM test compound was used to spike (1 μM) the donor buffer at physiologically relevant pH values (4 and 6.5), the donor plate slotted into the acceptor plate and incubated (4 h at room temperature) with gentle shaking (40-50 rpm). Following incubation, samples from the acceptor wells and theoretical equilibrium wells were transferred to the analysis plate and matrix matched with blank donor buffer. Acetonitrile containing internal standard (carbamazepine, 0.0236 μg/mL) was added to all samples and they were analyzed by LC-MS/MS (Agilent Rapid Resolution HPLC, AB SCIEX 4500 MS). The normalized (analyte/internal standard) peak areas were used to calculate the apparent permeability (P_{app}). Membrane integrity was assessed by calculating the P_{app} of Lucifer yellow (acceptable values <50 nM/s) using a Modulus microplate reader (excitation 490 nm/Emission 510-570 nm).[28]

Single point in vitro metabolic stability assay. The test compound (1 μM) was incubated at 37 °C in a solution containing 0.35 mg/ml microsomes (MLM; male Mouse BALB/c, Xenotech, or HLM, mixed gender, Xenotech) and metabolic reactions were initiated by the addition of NADPH (1 mM) in phosphate buffer (100 mM, pH 7.4), and incubated for 30 min. The samples were then prepared by cold-ice acetonitrile precipitation containing 0.1 μM carbamazepine (internal standard), centrifuged and filtered for LC-MS analysis. The incubation of compounds and controls (midazolam and MMV390048) were performed in triplicate. The relative loss of parent compound over the course of the incubation was monitored by LC-MS/MS and results reported as % remaining after 30 min incubation.

LC-MS/MS analyses were performed on a 4000 QTRAP® mass spectrometer (AB Sciex) equipped with a Turbo V™ ion source and coupled to an Agilent 1200 Rapid Resolution HPLC system (600 bar, Agilent technologies, USA). 2 μL of samples stored in a sample tray set at 8°C were injected onto a Kinetex C18 column, 2.1 mm x 50 mm, 2.6 μm

particles (Phenomenex) or Kinetex PFP column, 2.1 mm x 50 mm, 2.6 μm particles (Phenomenex) at 40 °C. Compounds were separated using a gradient solvent system consisting of 0.1% formic acid (A) and 0.1% formic acid in acetonitrile (B). MRM scans were operated under electrospray positive ionization mode and the operation parameters were as follows: curtain gas, 30 psi; nebulizer gas (GS1), 50 psi; turbo gas (GS2), 60 psi; source temperature, 500 °C; ion spray voltage, 5000 V; declustering potential and collision energy optimized from infusion of the compounds; collisional activated dissociation (CAD) gas setting: medium.

β-hematin Inhibition Assay. This assay quantifies the inhibition of β-hematin (synthetic hemozoin) formation at a particular drug concentration.[29] It involves addition of pyridine solution which complexes with free heme (detectable at an absorbance at 405 nm) but not β-hematin at the end of the reaction, allowing for quantification of β-hematin formation. Briefly, stock solutions of controls (CQ and AQ) and test compounds were made to 20 mM in DMSO. A solution containing water/305.5 μM NP40/DMSO at a v/v ratio of 70%/20%/10%, respectively was added to every well in columns 1-11 of a 96-well plate while 140 μL of water and 40 μL of 305.5 μM NP40 were added to column 12 to mediate the formation of β-hematin. Twenty microliters of control or test compound (20 mM) was added to column 12 and 100 μL of this solution serially diluted to column 2, with column 1 left as a blank (0 μM compound). A 178.8 μL aliquot of hematin stock was suspended in 20 mL of a 1 M acetate buffer, pH 4.9 and 100 μL of this hematin suspension added into each well. Plates were then incubated for ~5 h at 37 °C after which 32 μL of pyridine solution (20% water, 20% acetone, 10% 2 M HEPES buffer pH 7.4, 50% pyridine) was added followed by addition of 60 μL of acetone to all wells. Plates were read at 405 nm and dose-response curves plotted in GraphPad Prism v.6 (GraphPad Software Inc., La Jolla, USA) to obtain IC_{50}s.

Log*D* Determinations. For the determination of the distribution coefficient (Log*D*) between organic and aqueous phases at pH 5.0, compounds were evaluated by the shake-flask method at room temperature. Briefly, compounds were dissolved in DMSO to constitute 10 mM stock solutions. Each compound was then mixed in a glass tube with equal volumes of pre-saturated 0.02 M 2-(N-morpholino) ethanesulfonic acid (MES) buffer and *n*-octanol to achieve a final concentration of 75 μM. This solution was then shaken vigorously for 2 h, centrifuged at 3,500 rpm and allowed to equilibrate for 6 h. Each phase was then carefully separated and final drug concentrations in each layer determined by computing absorbance values measured with the extinction coefficients obtained from linear Beer's Law UV-vis spectroscopy plots in each phase within the concentration range tested. The concentrations in the two phases were used to obtain Log*D* at pH 5.0 using equation 3 shown below.

$$\mathbf{LogD_{5.0}} = \mathbf{Log}\ \frac{[\text{Compound in } n\text{-octanol}]\ \mu\text{M}}{[\text{Compound in MES buffer}]\ \mu\text{M}} \qquad \text{Equation 3}$$

For LogD measurements at pH 7.4, HPLC analysis was used instead since signal to noise ratio confounded UV-vis spectroscopic analysis of compound concentrations in the aqueous layer which were very low. In this analysis, a 10 mM stock solution of each compound was prepared in DMSO and 10 μL of this was used to spike a 1:1 mixture of phosphate buffered saline (pH 7.4) and *n*-octanol in a square-welled 96-deep-well plate. The solutions were shaken vigorously (1500 rpm) on an orbital shaker for 2 h at room temperature and thereafter, centrifuged (3500 rpm, 2700× *g*) in order to fully separate the two immiscible phases. Carefully, 300 μL from each layer was transferred to a new analysis plate and analysed on the HPLC-DAD (Agilent 1200 Rapid Resolution HPLC) with 0.1 % formic acid in 95 % acetonitrile as the organic mobile phase and 0.1 % formic acid in 5 % acetonitrile as the

aqueous mobile phase. $LogD_{7.4}$ was calculated from the areas of integrated UV chromatogram peaks using equation 4 below

$$\mathbf{LogD_{7.4}} = \mathbf{Log}\ \frac{\text{(peak area of } n\text{-octanol phase/}n\text{-octanol phase injected volume)}}{\text{(peak area of buffer phase/buffer phase injected volume)}} \quad \text{Eqn 4}$$

ASSOCIATED CONTENT

Supporting Information

The Supporting Information is available free of charge on the ACS Publications website at DOI:

SMILES file of compounds (Excel),

Cellular fractionation assay results

AUTHOR INFORMATION

Corresponding Author

*Phone: +27 (0)21 650 2528. E-mail: timothy.egan@uct.ac.za.

Notes

The authors declare no competing financial interest.

ACKNOWLEDGMENTS

This research was supported by the SAMRC (TJE) and The University of Cape Town, SAMRC, and South African Research Chairs Initiative of the Department of Science and Technology, administered through the South African National Research Foundation are gratefully acknowledged for support (K.C.). DT acknowledges the South African National Research Foundation for support through a Scarce Skills Postdoctoral fellowship (grant no. 85227). We acknowledge Nina Lawrence for assistance with ADME assays and Matthew Njoroge for assistance with metabolic stability and ID investigations.

ABBREVIATIONS USED

ACT: Artemisinin combination therapy; βHIA: β-hematin Inhibition activity; CHO cells: Chinese Hamster Ovarian cells; CQ: Chloroquine; CQS and CQR: Chloroquine –sensitive and resistant; DV: Digestive vacuole; hERG: human *Ether-a-Go-Go*-Related Gene; LAR: Lipid accumulation ratio; PfCRT: *Plasmodium falciparum* Chloroquine resistance transporter; PAMPA: Parallel Artificial Membrane Permeability Assay; RA: Reversal agent; RI: Resistance index; VAR: Vacuolar accumulation ratio

REFERENCES

1. Egan, T. J.; Ross, D. C.; Adams, P. A. Quinoline anti-malarial drugs inhibit spontaneous formation of b-haematin (malaria pigment). *FEBS Lett.* **1994,** *352*, 54-57.
2. Sullivan, D. J.; Gluzman, I. Y.; Russell, D. G.; Goldberg, D. E. On the molecular mechanism of chloroquine's antimalarial action. *Proc. Natl. Acad. Sci. U.S.A.* **1996,** *93*, 11865-11870.

3. Combrinck, J. M.; Mabotha, T. E.; Ncokazi, K. K.; Ambele, M. A.; Taylor, D.; Smith, P. J.; Hoppe, H. C.; Egan, T. J. Insights into the role of heme in the mechanism of action of antimalarials. *ACS Chem. Biol.* **2013,** *8*, 133-137.

4. Sidhu, A. b. S.; Verdier-Pinard, D.; Fidock, D. A. Chloroquine resistance in *Plasmodium falciparum* malaria parasites conferred by *pfcrt* mutations. *Science* **2002,** *298*, 210-213.

5. Bray, P. G.; Martin, R. E.; Tilley, L.; Ward, S. A.; Kirk, K.; Fidock, D. A. Defining the role of PfCRT in *Plasmodium falciparum* chloroquine resistance. *Mol. Microbiol.* **2005,** *56*, 323-333.

6. Noedl, H.; Se, Y.; Schaecher, K.; Smith, B. L.; Socheat, D.; Fukuda, M. M. Evidence of artemisinin-resistant malaria in western Cambodia. *N. Engl. J. Med.* **2008,** *359*, 2619-2620.

7. Dondorp, A. M.; Nosten, F.; Yi, P.; Das, D.; Phyo, A. P.; Tarning, J.; Lwin, K. M.; Ariey, F.; Hanpithakpong, W.; Lee, S. J.; Ringwald, P.; Silamut, K.; Imwong, M.; Chotivanich, K.; Lim, P.; Herdman, T.; An, S. S.; Yeung, S.; Singhasivanon, P.; Day, N. P. J.; Lindegardh, N.; Socheat, D.; White, N. J. Artemisinin resistance in *Plasmodium falciparum* malaria. *N. Engl. J. Med.* **2009,** *361*, 455-467.

8. Burgess, S. J.; Selzer, A.; Kelly, J. X.; Smilkstein, M. J.; Riscoe, M. K.; Peyton, D. H. A chloroquine-like molecule designed to reverse resistance in *Plasmodium falciparum*. *J. Med. Chem.* **2006,** *49*, 5623-5625.

9. Burgess, S. J.; Kelly, J. X.; Shomloo, S.; Wittlin, S.; Brun, R.; Liebmann, K.; Peyton, D. H. Synthesis, structure-activity relationship, and mode-of-action studies of antimalarial reversed chloroquine compounds. *J. Med. Chem.* **2010,** *53*, 6477-6489.

10. Andrews, S.; Burgess, S. J.; Skaalrud, D.; Kelly, J. X.; Peyton, D. H. Reversal agent and linker variants of reversed chloroquines: activities against *Plasmodium falciparum*. *J. Med. Chem.* **2010,** *53*, 916-919.

11. Joubert, J.; Fortuin, E. E.; Taylor, D.; Smith, P. J.; Malan, S. F. Pentacycloundecylamines and conjugates thereof as chemosensitizers and reversed chloroquine agents. *Bioorg. Med. Chem. Lett.* **2014,** *24*, 5516-5519.

12. October, N.; Watermeyer, N. D.; Yardley, V.; Egan, T. J.; Ncokazi, K. K.; Chibale, K. Reversed chloroquines based on the 3,4-dihydropyrimidin-2(1H)-one scaffold: synthesis and evaluation for antimalarial, beta-haematin inhibition, and cytotoxic activity. *ChemMedChem* **2008,** *3*, 1649-1653.

13. Musonda, C. C.; Whitlock, G. A.; Witty, M. J.; Brun, R.; Kaiser, M. Chloroquine-astemizole hybrids with potent in vitro and in vivo antiplasmodial activity. *Bioorg. Med. Chem. Lett.* **2009,** *19*, 481-484.

14. Kumar, A.; Srivastava, K.; Kumar, S. R.; Puri, S. K.; Chauhan, P. M. S. Synthesis of new 4-aminoquinolines and quinoline–acridine hybrids as antimalarial agents. *Bioorg. Med. Chem. Lett.* **2010,** *20*, 7059-7063.

15. Zishiri, V. K.; Joshi, M. C.; Hunter, R.; Chibale, K.; Smith, P. J.; Summers, R. L.; Martin, R. E.; Egan, T. J. Quinoline antimalarials containing a dibemethin group are active against chloroquinone-resistant *Plasmodium falciparum* and inhibit chloroquine transport via the *P. falciparum* chloroquine-resistance transporter (PfCRT). *J. Med. Chem.* **2011,** *54*, 6956-6968.

16. Kaschula, C. H.; Egan, T. J.; Hunter, R.; Basilico, N.; Parapini, S.; Taramelli, D.; Pasini, E.; Monti, D. Structure-activity relationships in 4-aminoquinoline antiplasmodials. The role of the group at the 7-position. *J. Med. Chem.* **2002,** *45*, 3531-3539.

17. Gleeson, P. M. Generation of a set of simple, interpretable ADMET rules of thumb. *J. Med. Chem.* **2008,** *51*, 817-834.

18. Zishiri, V. K.; Hunter, R.; Smith, P. J.; Taylor, D.; Summers, G.; Kirk, K.; Martin, R. E.; Egan, T. J. A series of structurally simple chloroquine chemosensitizing dibemethin derivatives that inhibit chloroquine transport by PfCRT. *Eur. J. Med. Chem.* **2011,** *46*, 1729-1742.

19. Warhurst, D. C.; Craig, J. C.; Adagu, I. S.; Guy, R. K.; Madrid, P. B.; Fivelman, Q. L. Activity of piperaquine and other 4-aminoquinoline antiplasmodial drugs against chloroquine-sensitive and resistant blood-stages of *Plasmodium falciparum*. Role of b-haematin inhibition and drug concentration in vacuolar water- and lipid-phases. *Biochem. Pharmacol.* **2007,** *73*, 1910-1926.

20. Warhurst, D. C.; Craig, J. C.; Adagu, I. S.; Meyer, D. J.; Lee, S. Y. The relationship of physico-chemical properties and structure to the differential antiplasmodial activity of the cinchona alkaloids. *Malaria J.* **2003,** *2,* 26.

21. Adjalley, S. H.; Scanfield, D.; Kozlowski, E.; Llinás, M.; Fidock, D. A. Genome-wide transcriptome profiling reveals functional networks involving the Plasmodium falciparum drug resistance transporters PfCRT and PfMDR1. *BMC Genomics* **2015,** *16*, 1090.

22. Combrinck, J. M.; Fong, K. Y.; Gibhard, L.; Smith, P. J.; Wright, D. W.; Egan, T. J. Optimization of a multi-well colorimetric assay to determine haem species in *Plasmodium falciparum* in the presence of anti-malarials. *Malaria J.* **2015,** *14*, e253.

23. Peters, W.; Robinson, B. L. In *Handbook of Animal Models*, Zak, O.; Sande, M., Eds. Academic: London, 1999; pp 757-773.

24. Hanaoka, K.; Muramatsu, Y.; Urano, Y.; Terai, T.; Nagano, T. Design and synthesis of a highly sensitive off–on fluorescent chemosensor for zinc Ions utilizing internal charge transfer. *Chem. Eur. J.* **2010,** *16*, 568-572.

25. Makler, M. T.; Ries, J. M.; Williams, J. A.; Bancroft, J. E.; Piper, R. C.; Gibbins, B. L.; Hinrichs, D. J. Parasite lactate dehydrogenase as an assay for *Plasmodium falciparum* drug sensitivity. *Am. J. Trop. Med. Hyg.* **1993,** *48*, 739-741.

26. Mosman, T. Rapid colorimetric assay for cellular growth and survival: application to proliferation and cytotoxicity assays. *J. Immunol. Methods* **1983,** *65*, 55-63.

27. Hill, A. P.; Young, R. J. Getting physical in drug discovery: A contemporary perspective on solubiity and hydrophobicity. *Drug Discovery Today.* **2010,** *15*, 648-655.

28. Wohnsland, F.; Faller, B. High-throughput permeability pH profile and high-throughput alkane/water log P with artificial membranes. *J. Med. Chem.* **2001,** *44*, 923-990.

29. Sandlin, R. D.; Carter, M. D.; Lee, P. J.; Auschwitz, J. M.; Leed, S. E.; Johnson, J. D.; Wright, D. W. Use of the NP-40 detergent-mediated assay in discovery of inhibitors of β-hematin crystallization. *Antimicr. Agents Chemother.* **2011,** *55*, 3363-3369.

Table of Contents graphic